Hindawi
Journal of Analytical Methods in Chemistry
Volume 2023, Article ID 8797355, 13 pages
https://doi.org/10.1155/2023/8797355

Research Article

Simultaneous Preconcentration of Fast Green FCF and Rhodamine B Using Deep Eutectic Solvent and Determination *via* High-Performance Thin Layer Chromatography

Forough Karami and Ardeshir Shokrollahi

Department of Chemistry, Yasouj University, Yasouj 75918-74831, Iran

Correspondence should be addressed to Ardeshir Shokrollahi; ashokrollahi@yu.ac.ir

Received 15 August 2023; Revised 4 November 2023; Accepted 14 November 2023; Published 4 December 2023

Academic Editor: Fábio R. P. Rocha

The aim of the current investigation is the development of a green, quick, easy, and accurate method for simultaneous preconcentration of fast green FCF (FG) and rhodamine B (Rh B) using a deep eutectic solvent (DES). Then, the high-performance thin layer chromatography (HPTLC) technique was used for the determination of analytes. Decanoic acid and tetrabutylammonium bromide were chosen as the components of DES. HPTLC analysis was performed on an aluminum plate silica gel 60 F_{254}. Methanol-ammonia and ethyl acetate were selected as the mobile phase. Scanning of the plates was accomplished by scanner 3. Effective parameters on the preconcentration process such as concentration of salt, volume of DES, stirrer time, and pH were investigated *via* central composite design (CCD). Data validation demonstrated good repeatability. The limit of detection for FG and Rh B was obtained as 0.08 and 0.01 $\mu g \cdot mL^{-1}$, respectively. The enrichment factor for FG and Rh B was achieved as 7.43 and 10.77, respectively. The linear ranges for FG and Rh B were acquired as 0.10–1.20 and 0.05–1.20 $\mu g \cdot mL^{-1}$, respectively. The preconcentration factor for both analytes was 21.66. Finally, the proposed method was successfully used for the quantitation of FG and Rh B in pastille and lipstick.

1. Introduction

Synthetic dyes have drawn considerable attention in different industries including food, paper, medicine, textile, and cosmetic [1] because of low cost and favorable appearance. In general, synthetic pigments influence psychological effects, which lead to loss of control, crying, increased sleeplessness, and other diseases [2]. Of these approaches, the consumption of food dyes in different applications should be limited. Rhodamine B (Rh B) as one of the synthetic dyes is known as a harmful compound for human health and used in various industries such as food, leather, textile, paper, printing, and plastic [3]. Due to the carcinogenic effects of Rh B on the eyes, skin, and liver, it is banned for use in the food industry [4, 5]. Fast green FCF (FG) as another synthetic dye is extensively used in the coating of candy, beverages, ice cream, health, and skin care products [6]. The toxicity and allergenic effects of FG had been published [7, 8]. It may also cause irritation of the eyes and skin [8].

Direct quantitation of FG and Rh B without specific pretreatment is problematic because of the matrix effects of other components and their low amounts in real samples. Therefore, preconcentration methods have been applied when it is difficult to detect trace amounts of analytes. The miniaturized form of liquid-liquid extraction entitled as liquid-phase microextraction (LPME) uses microliter volume to provide high extraction efficiency. LPME has some advantages such as economic extraction, rapid phase transportation, high capacity of extraction, and the facility of direct injection of samples into analytical instruments [9]. Numerous extraction methods including magnetic solid phase extraction [10, 11], solid phase microextraction [12, 13], hollow fiber liquid phase microextraction [14, 15],

single drop microextraction [16], dispersive liquid-liquid microextraction [17], ultrasound-assisted LPME [18], and liquid-liquid microextraction [19, 20] had been reported for the extraction and determination of synthetic dyes. In recent years, there has been an increasing focus on the utilization of deep eutectic solvents (DESs) as a novel green solvent. These solvents were first introduced by Abbott et al. in 2004 [21]. DESs are made *via* the combination of a hydrogen bond acceptor (HBA) and a hydrogen bond donor (HBD) due to the formation of hydrogen bonds after heating at a temperature of 60–90°C for 30 min to one hour [21]. The melting point of DES is lower than that of its constitutive component [22]. Some properties of DES including the degree of affinity for target components, less solubility, and good dispersion in aqueous media influence the extraction methodology [23]. DESs have been extensively used for extraction, separation, and preconcentration processes [24].

Numerous compounds have been proposed for the synthesis of DES. For instance, choline chloride or vitamin B_4 is introduced as the most used HBA, whereas amino acids, carboxylic acids, urea, ethylene glycol, glycerol, and sugars have been used as HBD [24]. DESs show the characteristic of high purity and eco-friendly [25], which have been used for the extraction and microextraction of synthetic dyes: simultaneous identification of eight synthetic dyes [26], determination of some red dyes [27], and determination of sunset yellow dye [28].

Various techniques have been proposed for the analysis of dyes such as spectroscopy [19, 29], high-performance liquid chromatography [30, 31], high-performance liquid chromatography-mass spectrometry [32], scanometry [33, 34], and thin layer chromatography (TLC) [35]. Among the different analytical techniques, high-performance thin layer chromatography (HPTLC) is known as a low cost, simple, and rapid technique that is appropriate for the comparison and separation of different components [36]. HPTLC has numerous advantages over other methods: simultaneous study of different compounds, automation, less solvent compared to other liquid chromatography methods, easy pretreatment, fast, and cheap analysis [37, 38]. Therefore, it can be considered as a green analytical technique [39].

As mentioned above, it is vital to use extraction systems employing environmentally friendly solvents to reduce the consumption of hazardous organic materials. Thus, in this investigation, a DES based on the combination of decanoic acid (DA) as a HBD and tetrabutylammonium bromide (TBAB) as a HBA was used for the simultaneous preconcentration of two synthetic dyes followed by HPTLC technique as the modern analytical instrument of TLC for the determination of dyes, which is a reliable and cost-effective technique. Additionally, central composite design (CCD) was applied as an efficient method to study the interactions between effective parameters and system response. The developed analysis is innovative in terms of the methodology for the simultaneous quantitation of artificial dyes and the used solvent for the extraction process.

2. Materials and Methods

2.1. Materials and Instruments. All chemicals and reagents were of analytical grade. DA, TBAB, sodium chloride, FG, Rh B, Quinoline Yellow, tartrazine, methanol (MeOH), acetonitrile (ACN), ethanol, ethyl acetate, ammonia, and aluminum plate silica gel 60 F_{254} (20×20 cm) were purchased from Merck Company (Darmstadt, Germany).

Agilent Technologies Cary Series 100 UV/VIS Spectrophotometer was used for spectra acquisition. The chromatographic analyses were performed by Camag HPTLC, made in Switzerland, equipped with ATS4, scanner 3, and visualizer.

2.2. Preparation of DES. DES was prepared according to our previous report [40]. In brief, 2 mmol DA and 1 mmol TBAB were mixed and stirred at a temperature of 50°C until a clear liquid was attained (about 30 min).

2.3. Preconcentration Process. Stock solutions of FG and Rh B (1×10^{-2} mg·mL^{-1}) were prepared in MeOH. To survey the preconcentration of dyes, different concentrations of sodium chloride, volume of DES, stirrer time, and pH were studied using CCD by the software package Design-Expert version 7.0.0 trial. The effective factors and condition of levels are presented in Tables 1 and 2, respectively. For each level, in a Falcon tube (15 mL), a definite concentration of salt (according to Table 2, for example, 0.350 mol·L^{-1}) was mixed with distinctive volume of dyes 1×10^{-2} mg·mL^{-1} (according to Table 2, for example, 390 μL) and the solution was made up to 13 mL *via* deionized water. Then, adjusting pH (according to Table 2, for example, 4.50) was performed and an appropriate volume of DES (according to Table 2, for example, 375 μL) was added to the Falcon tube. In the following, the mixture was stirred at desired time (according to Table 2, for example, 15 min). After finishing the stirrer time, the solution was centrifuged at 4000 rpm for 5 min. Next, the Falcon tubes were inserted in an ice beaker, resulting in the formation of a solid and thin layer on top of the solution, which was related to the preconcentrated dyes. This layer was separated using a spatula and diluted using MeOH before HPTLC analysis. The schematic preparation of this procedure is presented in Scheme 1.

2.4. Preparation of Real Samples. Lipstick and pastille were purchased from Shiraz City, Fars Province, Iran. The preparation of lipstick was carried out based on Yilmaz's et al. investigation with a little modification [29]. In brief, 0.899 g of lipstick was weighed in a 50 mL Falcon tube and 10 mL of ethanol was added. The sample was vortexed for 1 min, ultrasonicated for 30 min, and centrifuged for 20 min at 4000 rpm. In the next step, the supernatant was collected, diluted with a dilution factor of 50, and kept in a refrigerator for further experiments. In the following, 1.3 g of pastille was dissolved in 6 mL of deionized water. The solution was vortexed for 1 min, ultrasonicated for 30 min at a temperature of 70°C, and filtered using a PTFE filter.

Table 1: Effective factors and limit of levels for response surface quadratic model.

Factor	$-\alpha$	-1	0	$+1$	$+\alpha$
pH	2.10	3.30	4.55	5.70	6.90
Concentration of sodium chloride (mol L^{-1})	0.00	0.18	0.35	0.53	0.70
Volume of deep eutectic solvent (μL)	225	300	375	450	525
Stirrer time (min)	5	10	15	20	25

Table 2: Experimental conditions from central composite design analysis for the simultaneous preconcentration of fast green FCF and rhodamine B.

Run	pH	Volume of deep eutectic solvent (μL)	Concentration of salt (mol L^{-1})	Stirrer time (min)
1	6.90	375	0.35	15
2	4.50	375	0.35	5
3	4.50	225	0.35	15
4	3.30	300	0.53	10
5	3.30	300	0.53	20
6	4.50	375	0.35	15
7	4.50	375	0.35	15
8	4.50	375	0.35	15
9	4.50	375	0.35	15
10	4.50	375	0.00	15
11	3.30	450	0.53	20
12	5.70	450	0.53	20
13	4.50	375	0.35	15
14	3.30	450	0.18	20
15	5.70	450	0.18	10
16	3.30	450	0.53	10
17	5.70	450	0.53	10
18	5.70	300	0.18	20
19	4.50	525	0.35	15
20	4.50	375	0.70	15
21	5.70	300	0.53	20
22	5.70	450	0.18	20
23	5.70	300	0.18	10
24	2.10	375	0.35	15
25	3.30	300	0.18	20
26	5.70	300	0.53	10
27	3.30	450	0.18	10
28	4.50	375	0.35	25
29	4.50	375	0.35	15
30	3.30	300	0.18	10

2.5. Preconcentration of Real Samples. To extract chosen dyes using DES from real samples, 390 μL of lipstick (diluted solution) and 600 μL of supernatant solution of pastille were transferred to a Falcon tube. Then, 2.3 mL of NaCl (2 mol·L^{-1}) was added and after dilution using deionized water (13 mL), the pH of solution was adjusted (pH 4.64). Afterward, 378 μL of synthesized DES was added to the tube and the solution was stirred for 15 min. For the separation of phases, centrifugation was done at 4000 rpm for 5 min. In the following, the Falcon tube was kept in an ice beaker, which resulted in the separation of organic phase containing extracted dyes. Due to the high viscosity of DES, the obtained extraction phase was diluted by MeOH (600 μL) before HPTLC analysis.

2.6. Instrumental Conditions. Chromatographic analysis at room temperature and 20% humidity was accomplished by Camag HPTLC, made in Switzerland, equipped with ATS4, scanner 3, and visualizer. Before each analysis, the plate was washed using MeOH to remove any contamination. The preconcentrated dyes, in the form of band, were spotted by ATS4 under N_2 gas (5 bar pressure) on an aluminum plate silica gel 60 F_{254} (20 × 20 cm) with a band length of 9 mm and a distance of 13.5 mm. 2.5 and 5 μL of preconcentrated and standard dyes were applied, respectively. Developing of the plates was done manually under the following conditions: MeOH-ammonia and ethyl acetate with a ratio of 20-20 and 60% v/v, respectively, as the mobile phase; chamber saturation time,

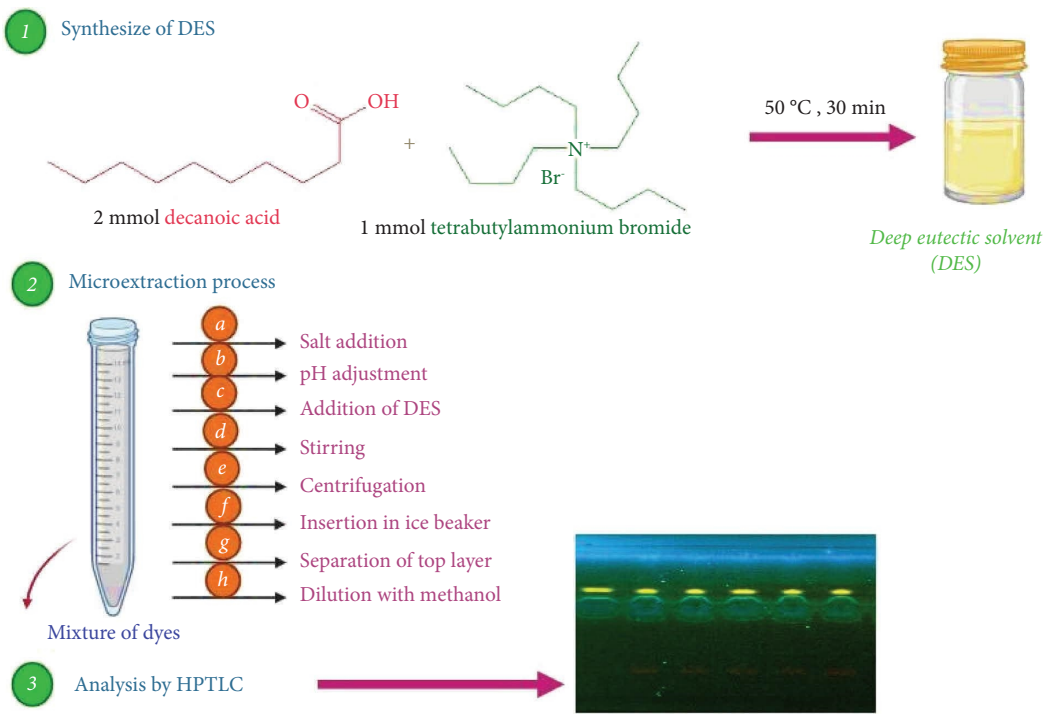

Scheme 1: Schematic illustration of preconcentration procedure.

20.0 min; volume of mobile phase, 10 mL; and migration distance, 90 mm. Scanning of the plates was performed by scanner 3 to the following conditions: the wavelength of 620 nm and absorption mode for FG; the wavelength of 365 nm and fluorescence mode for Rh B; slit dimension, 6.00 mm × 0.40 mm, macro; scanning speed, 20 mm/s; data resolution, 100 μm/step; lamp W for FG; lamp Hg for Rh B. Finally, the image of plates was obtained by the visualizer at 366 nm and visible wavelengths. Recording of data was carried out *via* WinCATS software.

3. Results and Discussion

3.1. Optimization of Chromatographic Conditions. It is vital to improve some significant parameters including the volume of spots, time of tank saturation, type of mobile phase, migrating distance of solvent, and detection wavelength of analytes using HPTLC technique [41]. In the current research, among different spot volumes that had been loaded on an aluminum silica gel plate, the volumes of 2.5 and 5 μL for preconcentrated and standard dyes, respectively, were applied, which yielded the narrow bands. Also, among various band lengths (6, 8, and 9 mm), the band length of 9 mm was selected, which resulted in an appropriate band. In order to find a mobile phase that can separate two analytes with a good R_f, seventeen different mobile phases were investigated, which are described in Table 3. Finally, the best simultaneous separation for dyes of FG and Rh B was achieved using MeOH (20% v/v)-ammonia (20% v/v) and ethyl acetate (60% v/v) that resulted in R_f values of 0.11 and 0.70 for FG and Rh B, respectively. Before each analysis, tank saturation, as a main factor in planar chromatography, was performed for 20 min providing a uniform atmosphere to achieve equilibration for separation. Increasing the migration distance of solvent resulted in high resolution. Therefore, the solvent distance of 90 mm was chosen to obtain a good resolution. The HPTLC images of preconcentrated dyes are shown in Figure 1.

UV-VIS spectra of selected dyes were obtained using a spectrophotometer for spectra acquisition of FG and Rh B. By doing so, the detection of FG was carried out in an absorption mode at the maximum wavelength of the dye (620 nm). For the detection of Rh B, at first, scanner 3 was adjusted at the maximum wavelength of dye (545 nm) in an absorption mode, which formed an inappropriate signal. Hence, due to the fluorescence properties of Rh B, scanning of the plates was performed in fluorescence mode. The densitograms of preconcentrated FG in absorption mode at 620 nm and Rh B in fluorescence mode at 365 nm are presented in Figure 2. As shown in Figure 1, FG and Rh B were distinctly detected as red and yellow colours under 365 nm, respectively. Similarly, under visible light, FG and Rh B were separately identified as blue and pink spots, respectively. So, there is no interference between analytes.

3.2. Central Composite Design. As presented in Table 1, a CCD was applied to adjust four effective parameters including pH, concentration of salt, volume of DES, and stirrer time. 30 experiments were done based on the experimental design. Characteristics of each level are shown in Table 2. Analysis of variance (ANOVA) shown in Table 4 expresses the significance of designed model and the main interactions among variables. The amounts of F value (Table 4) show that the model for two dyes is significant.

Table 3: Various mobile phases for simultaneous separation of fast green FCF and rhodamine B.

Number	Solvent system
1	Ethyl acetate (6.1 mL), methanol (2 mL), ammonia (0.925 mL), and deionized water (0.925 mL)
2	Ethyl acetate (6.1 mL), methanol (2 mL), and ammonia (0.925 mL)
3	Ethyl acetate (6.1 mL) and methanol (2 mL)
4	Ethyl acetate (6.1 mL), methanol (2 mL), formic acid (0.925 mL), and deionized water (0.925 mL)
5	Ethyl acetate (7.1 mL), methanol (1 mL), formic acid (0.925 mL), and deionized water (0.500 mL)
6	Ethyl acetate (7.1 mL), methanol (1.5 mL), formic acid (0.925 mL), and deionized water (0.500 mL)
7	Ethyl acetate (6.5 mL), methanol (2.5 mL), and formic acid (0.500 mL)
8	Ethyl acetate (8 mL) and formic acid (2 mL)
9	Ethyl acetate (6 mL), methanol (2 mL), and acetic acid (0.500 mL)
10	Ethyl acetate (6.1 mL), acetone (1 mL), ammonia (0.925 mL), and deionized water (0.925 mL)
11	Ethyl acetate (6.1 mL), acetone (3 mL), and formic acid (0.500 mL)
12	Ethyl acetate (9 mL), acetone (1 mL), ammonia (0.500 mL), and deionized water (0.200 mL)
13	Ethyl acetate (9.5 mL), acetone (0.500 mL), and formic acid (0.500 mL)
14	Ethyl acetate (9 mL), acetone (1 mL), and methanol (0.500 mL)
15	Ethyl acetate (9 mL), acetone (1 mL), methanol (0.500 mL), and deionized water (0.200 mL)
16	Ethyl acetate (6.1 mL), methanol (2 mL), and formic acid (0.925 mL)
17	**Ethyl acetate (6 mL), methanol (2 mL), and ammonia (2 mL)**

The bold value is used for the simultaneous separation of fast green FCF and rhodamine B.

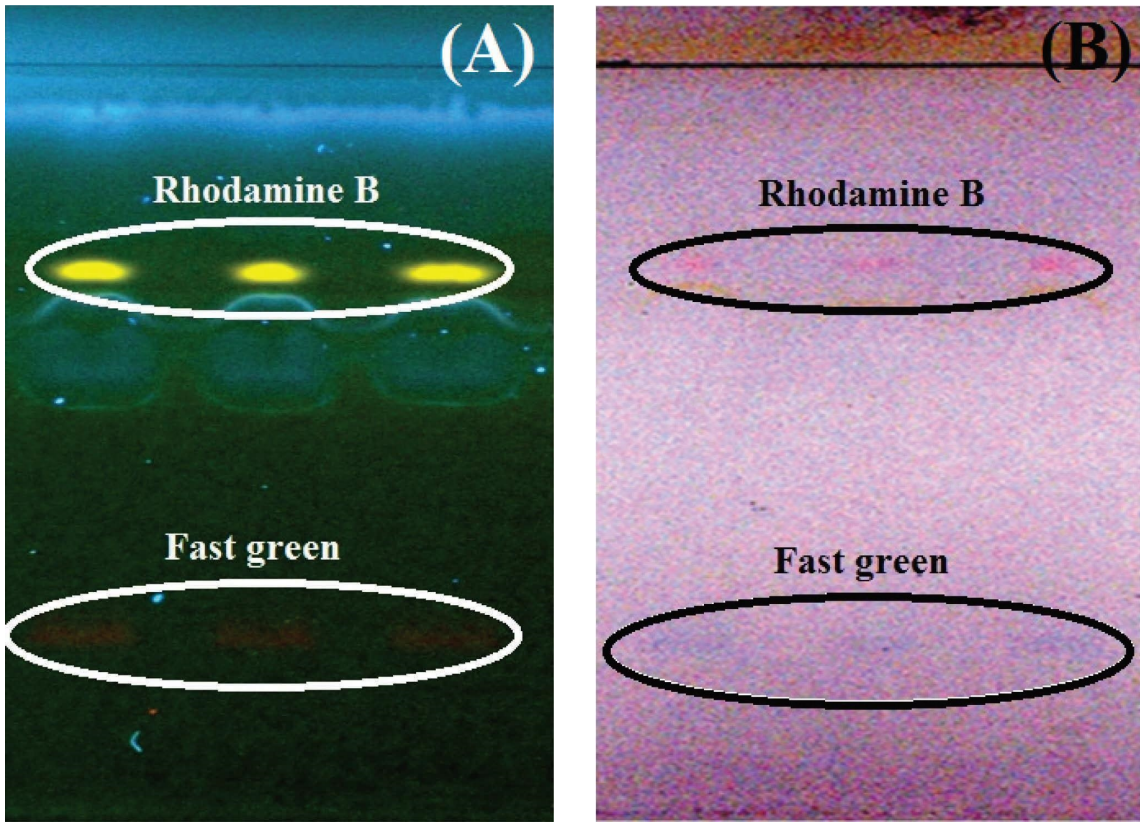

Figure 1: High-performance thin layer chromatography images of preconcentrated fast green FCF and rhodamine B using deep eutectic solvent. (A) Under UV 366 nm. (B) Under visible light.

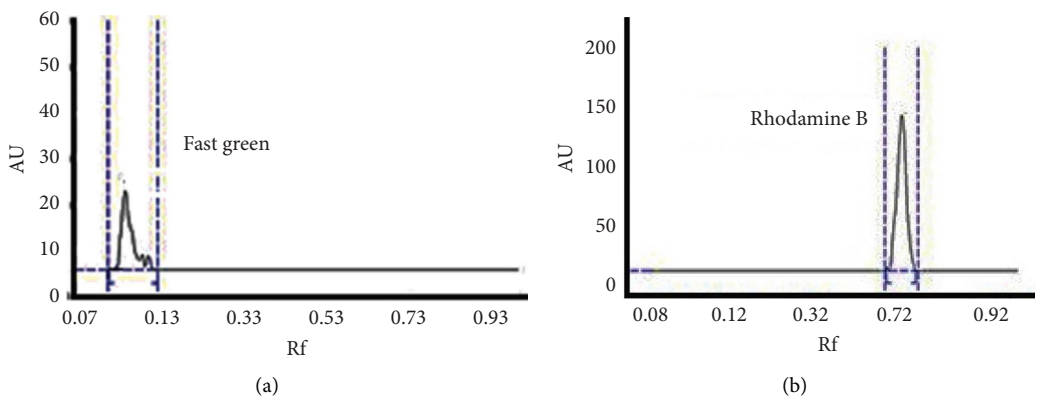

Figure 2: Densitograms of preconcentrated dyes. (a) Fast green FCF in absorption mode at 620 nm. (b) Rhodamine B in fluorescence mode at 365 nm.

Table 4: Analysis of variance results for simultaneous preconcentration of fast green FCF and rhodamine B.

Source	Sum of squares	D.F[1]	Mean square	F value	p value	
Fast green FCF						
Model	$8.629E+006$	14	$6.164E+005$	956.71	<0.0001	Significant
A (pH)	8719.19	1	8719.19	13.53	0.0022	
B (volume of deep eutectic solvent)	$1.78E+05$	1	$1.78E+05$	276.54	<0.0001	
C (concentration of salt)	$6.37E+05$	1	$6.37E+05$	988.59	<0.0001	
D (stirrer time)	21090.05	1	21090.05	32.73	<0.0001	
AB	96744.33	1	96744.33	150.16	<0.0001	
AC	196.35	1	196.35	0.3	0.589	
AD	20653.28	1	20653.28	32.06	<0.0001	
BC	$5.70E+05$	1	$5.70E+05$	885.37	<0.0001	
BD	21035.88	1	21035.88	32.65	<0.0001	
CD	899.25	1	899.25	1.4	0.2558	
A^2	$2.77E+06$	1	$2.77E+06$	4303.69	<0.0001	
B^2	$1.68E+06$	1	$1.68E+06$	2601.86	<0.0001	
C^2	$6.36E+05$	1	$6.36E+05$	986.39	<0.0001	
D^2	$4.41E+06$	1	$4.41E+06$	6844.58	<0.0001	
Residual	9664.09	15	644.27			
Lack of fit	8347.39	10	834.74	3.17	0.1074	Not significant
Pure error	1316.7	5	263.34			
Total	$8.64E+06$	29				
Rhodamine B						
Model	$8.455E+006$	14	$6.039E+005$	455.35	<0.0001	Significant
A (pH)	$1.107E+005$	1	$1.107E+005$	83.47	<0.0001	
B (volume of deep eutectic solvent)	$1.10E+05$	1	$1.10E+05$	82.8	<0.0001	
C (concentration of salt)	$9.64E+05$	1	$9.64E+05$	727.06	<0.0001	
D (stirrer time)	68.01	1	68.01	0.051	0.8239	
AB	$1.70E+05$	1	$1.70E+05$	128.07	<0.0001	
AC	98863.08	1	98863.08	74.54	<0.0001	
AD	1434.52	1	1434.52	1.08	0.3148	
BC	$3.77E+05$	1	$3.77E+05$	284.38	<0.0001	
BD	$5.29E+05$	1	$5.29E+05$	398.98	<0.0001	
CD	$1.77E+05$	1	$1.77E+05$	133.09	<0.0001	
A^2	$2.06E+05$	1	$2.06E+05$	155.14	<0.0001	
B^2	$2.79E+06$	1	$2.79E+06$	2103.05	<0.0001	
C^2	$1.16E+05$	1	$1.16E+05$	87.35	<0.0001	
D^2	$3.25E+06$	1	$3.25E+06$	2447.51	<0.0001	
Residual	19893.5	15	1326.23			
Lack of fit	11130.83	10	1113.08	0.64	0.7472	Not significant
Pure error	8762.67	5	1752.53			
Total	$8.47E+06$	29				

[1]Degree of freedom.

ANOVA data for FG were obtained as follows: values of p value less than 0.0500 indicate that the model terms are significant. In this case, A, B, C, D, AB, AD, BC, BD, A^2, B^2, C^2, and D^2 are significant terms. The F value for Lack of Fit (3.17) implies that the Lack of Fit is not significant relative to the pure error. The predicted R-Squared of 0.9942 is in agreement with the adjusted R-Squared of 0.9978 (Table 5) and shows a high dependence and correlation between the achieved and expected values of response. High value of adequate precision as the signal to noise ratio is desirable. Hence, the value of 92.664 indicates an adequate signal.

Table 5: The values of R^2 from central composite design analysis for fast green FCF and rhodamine B.

Values of R^2	Fast green FCF	Rhodamine B
R-squared	0.9989	0.9977
Adjusted R-squared	0.9978	0.9955
Predicted R-squared	0.9942	0.9909
Adequate precision	92.664	89.016

Finally, a quadratic equation is achieved *via* the coefficient values, which is as follows:

$$R_{FG} = 1888.66 + 19.06\,A + 86.16\,B - 162.91\,C - 29.64\,D + 77.76\,AB - 3.50\,AC + 35.93\,AD + 188.82\,BC + 36.26\,BD + 7.50\,CD - 317.95\,A^2 - 247.22\,B^2 - 152.22\,C^2 - 400.97\,D^2, \quad (1)$$

where R_{FG} is the area of FG and A, B, C, D are considered as the pH of mixture, volume of DES, concentration of salt, and stirrer time, respectively.

Similarly, ANOVA data for Rh B were achieved as follows: values of p value less than 0.0500 indicate that the model terms are significant. In this case, A, B, C, AB, AC, BC, BD, CD, A^2, B^2, C^2, and D^2 are significant terms. The F value for Lack of Fit (0.64) implies that the Lack of Fit is not significant relative to the pure error. The predicted R-Squared of 0.9909 is in agreement with the adjusted R-Squared of 0.9955 (Table 5). High amounts of R^2 (Table 5) approve that there is a high correlation between the expected and experimental data [42]. A high value of adequate precision (89.016) indicates an adequate signal. Finally, a quadratic equation is achieved *via* the coefficient values, which is as follows:

$$R_{RhB} = 2361.97 + 67.92\,A - 67.64\,B + 200.44\,C + 1.68\,D + 103.03\,AB - 78.61\,AC - 9.47\,AD + 153.53\,BC - 181.86\,BD + 105.03\,CD - 86.61\,A^2 - 318.88\,B^2 + 64.99\,C^2 - 344.01\,D^2. \quad (2)$$

In order to understand the acquired results, the graphs of three-dimensional response surface are shown in Figure 3. To find the best response, the desirability parameter of 1.0 was selected as the maximum response. Of these approaches, the pH value of 4.64, salt concentration of 0.35 mol·L^{-1}, DES volume of 378 μL, and stirrer time of 15 min were chosen as the optimum points.

3.3. Optimization of Variables. As mentioned before, a CCD was applied for preconcentration of two dyes to acquire the best conditions and assay the main variables and their interactions. As depicted in Figure 3, the volume of DES in the preconcentration of selected dyes was studied in a range of 225–525 μL by CCD. Because of the satisfactory properties of DESs, they have been extensively applied instead of conventional organic solvents and ionic liquids in the extraction, separation, and preconcentration processes [43]. An appropriate extraction agent in liquid phase microextraction processes plays a significant effect for the effective separation of analytes because the DES provides a stable phase (due to nonvolatile solvent), which improves the extraction efficiency [22]. Moreover, in liquid phase microextraction methods, the volume of extraction agent (solvent) is considered as one of the most significant factors, which extremely affected the extraction efficiency and preconcentration factor [22]. In the current investigation, high amounts of DES lead to a significant response because of increasing droplets of DES. Meanwhile, a low volume of DES reduces extraction efficiency, probably due to the decrease in DES droplets making insufficient separation. It seems that when the volume of solvent is high, the available droplets are more resulting in an increase of interaction between two phases.

The application of an inorganic salt affects the extraction efficiency [44]. This is because it causes variations in ionic strength and provides an inert medium that is suitable for the extraction process. In the current study, the concentration of sodium chloride (as the salt) was investigated in the range of 0.0–0.7 mol·L^{-1}. As presented in Figure 3, a low signal was detected, when no salt was used. The reason for this is that the DES cannot be absolutely removed from the solution [44]; therefore, small amounts of analytes are collected and extraction efficiency will decrease. Also, high concentration of sodium chloride can reduce the extraction efficiency, maybe due to the decrease in distribution coefficients of the target compounds that can change the ionic strength of the solution [44]. Thus, the concentration of 0.35 mol·L^{-1} was selected to achieve good separation.

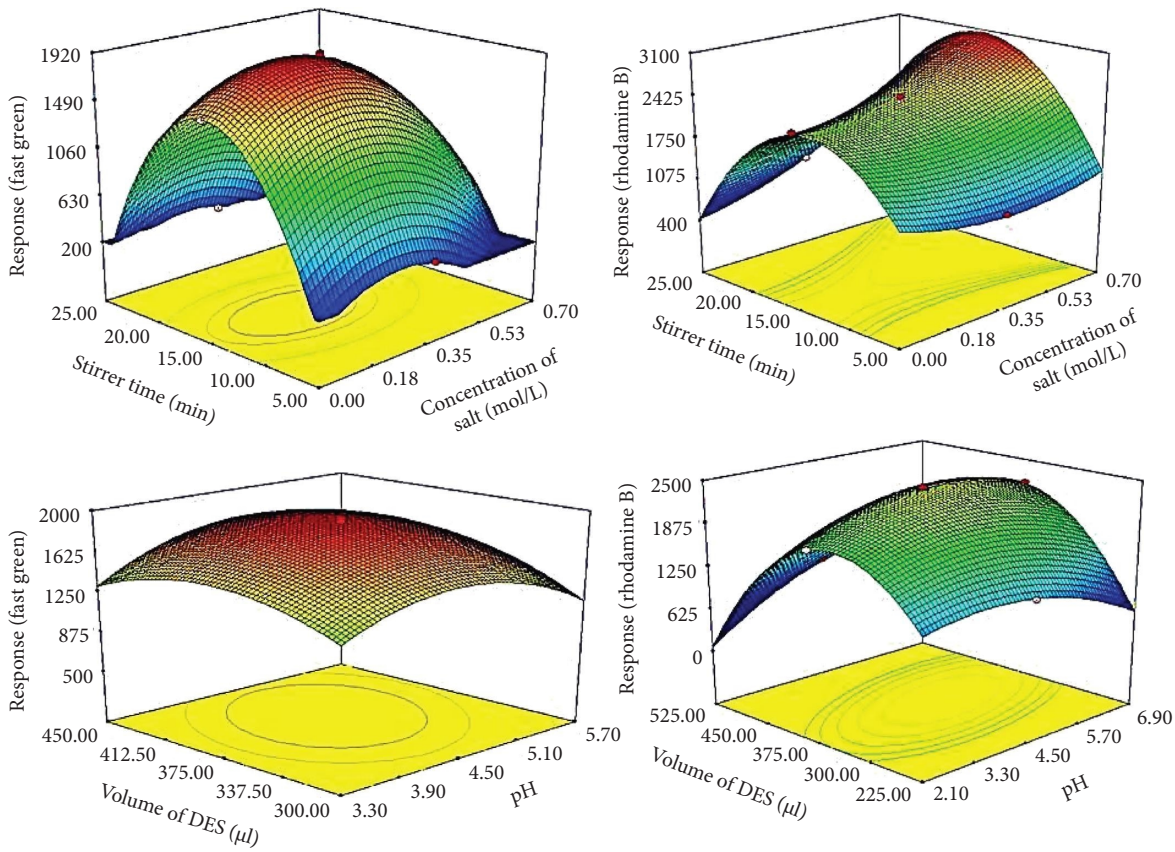

Figure 3: Three-dimensional response surface graphs for simultaneous preconcentration of fast green FCF and rhodamine B.

Table 6: Analytical parameters for simultaneous determination of fast green FCF and rhodamine B based on deep eutectic solvent.

Name	Calibration equation	Linear range (μg mL^{-1})	LOD (μg mL^{-1})	r	EF	PF	Repeatability (%)
Fast green FCF	$Y = 664.66\ X + 160.44$	0.10–1.20	0.08	0.998	7.43	21.66	3.65
Rhodamine B	$Y = 2922.5\ X + 290.29$	0.05–1.20	0.01	0.998	10.77	21.66	3.47

LOD: limit of detection; r: correlation coefficient; EF: enrichment factor; PF: preconcentration factor.

In an extraction process, pH is an essential parameter, which can increase extraction efficiency. In the current research, the effect of pH was investigated in a range of 2.10–6.91 by CCD. At acidic media, the carboxylic group of Rh B ($pK_a = 4.1$) [45] is not ionizing and approximately forms a neutral molecule, which leads to pass from the aqueous phase to the extraction phase and results in high efficiency [29]. At low acidic pH for FG, the anionic groups of SO_3^- convert to the neutral form (SO_3H) resulting in high extraction efficiency. In addition, the presence of DA ($pK_a = 4.9$) and salt makes approximately an inert medium, which is suitable for an effective extraction.

Another investigated parameter was stirrer time, which was studied in the range of 5–25 min. The amount of stirrer time between DES and analyte solution influences the extraction efficiency due to providing a mass transfer of the target compound from aqueous media to the extraction phase and also formation of a good emulsification [22]. When the phases of organic and inorganic are mixed at high stirrer time, a partial separation of two phases happens, which results in decreasing extraction efficiency [42]. Consequently, the stirrer time of 15 min was achieved as the best contact time.

According to the presented reasons above, the pH value of 4.64, salt concentration of 0.35 mol·L^{-1}, DES volume of 378 μL, and stirrer time of 15 min as the best conditions for simultaneous preconcentration of FG and Rh B were proposed by CCD.

3.4. Method Validation. Validation of an analytical method is important to confirm the reliability and suitability of a designed method [46]. Therefore, the figures of merit such as linear range, calibration curve, correlation coefficient (r), limit of detection (LOD), preconcentration factor (PF) [34], enrichment factor (EF) [34], and repeatability were investigated under the optimized conditions as presented in Table 6. Calibration curves of the two dyes were plotted

Table 7: Determination of fast green FCF and rhodamine B in real samples *via* standard addition method.

Type of sample	Analyte	Added amount (μg·mL^{-1})	Found amount ($n = 3$, μg·mL^{-1})	Recovery (%)
Pastille	Fast green FCF	0.00	0.35 ± 0.01	—
	Rhodamine B	0.00	—	—
	Fast green FCF	0.20	0.58 ± 0.01	115.00
	Rhodamine B	0.05	0.047 ± 0.01	94.00
	Fast green FCF	0.40	0.81 ± 0.01	115.00
	Rhodamine B	0.15	0.11 ± 0.01	73.33
Lipstick	Rhodamine B	0.00	0.05 ± 0.01	—
	Fast green FCF	0.00	—	—
	Rhodamine B	0.40	0.48 ± 0.04	107.50
	Fast green FCF	0.25	0.26 ± 0.02	104.00
	Rhodamine B	0.80	0.96 ± 0.02	113.75
	Fast green FCF	0.45	0.43 ± 0.01	95.55

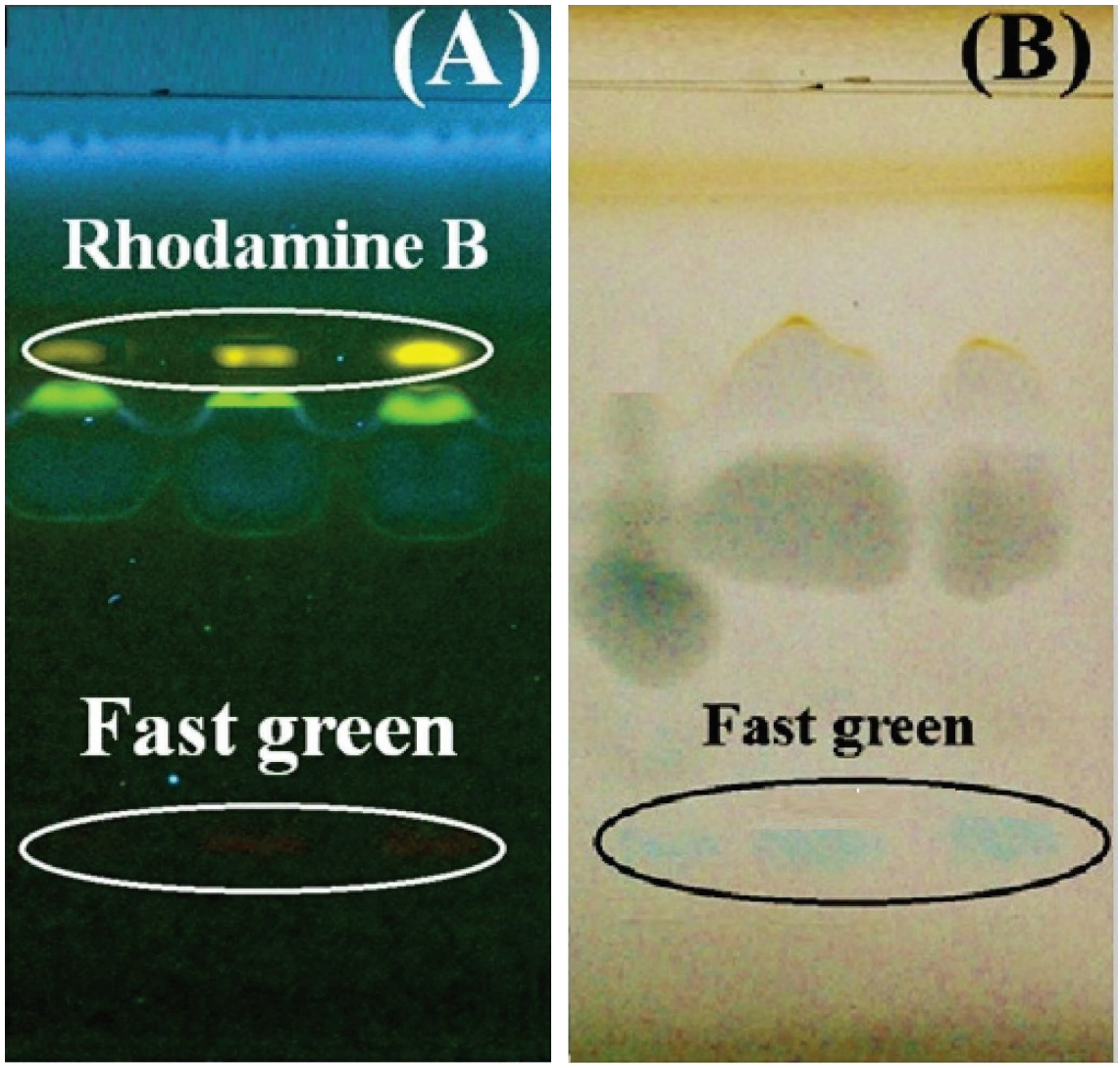

Figure 4: High-performance thin layer chromatography images of fast green FCF and rhodamine B. (A) Lipstick at the wavelength of 366 nm. (B) Pastille at visible light.

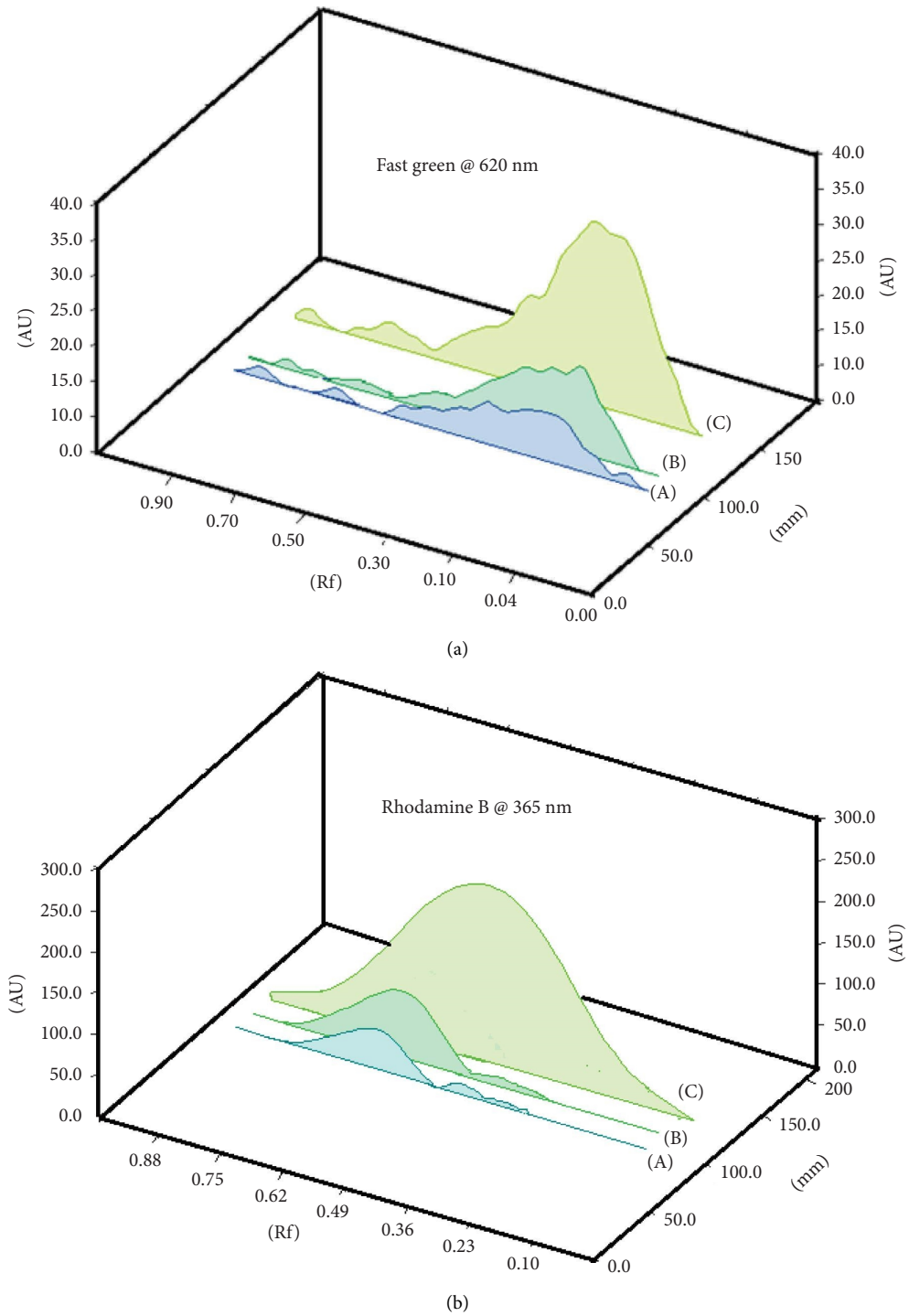

Figure 5: Three-dimensional chromatograms of (a) fast green FCF in pastille and (b) rhodamine B in lipstick. (A), (B), and (C) are related to different concentrations of analytes based on the standard addition method.

using the peak areas of FG and Rh B against desired concentrations in definite ranges. High correlation coefficient for the two dyes ($r = 0.998$) indicated good linearity. The practical LODs of 0.08 μg·mL^{-1} for FG and 0.01 μg·mL^{-1} for Rh B were measured at the lowest amount of dyes to be indicated. The repeatability parameter, indicating the precision of the method, for FG and Rh B was calculated as the relative standard deviation percent (RSD %) for five replicate determinations of a definite concentration. The parameters of PF and EF were evaluated under the optimized conditions based on the equations of 3 and 4, respectively [40]. The value of PF (21.66 for both dyes) in an extraction process indicates that how much the analyte has been concentrated. A higher value of PF shows a more efficient extraction, which

Table 8: Comparison of the proposed method with other analytical techniques for the determination of fast green FCF and rhodamine B.

Analyte	Preconcentration factor	RSD (%)	Analytical technique	References
FG	15	1.52	CPE-UV-VIS spectrophotometry	[33]
Rh B	8.5	2.40	CPE-UV–VIS spectrophotometry	[47]
Rh B	100	0.87	HPLC	[48]
Rh B	25	2.3	UV-VIS spectrophotometry	[29]
FG	21.66	3.65	DES-HPTLC	Current research
Rh B	21.66	3.47	DES-HPTLC	Current research

CPE: cloud point extraction, DES: deep eutectic solvent, FG: fast green FCF, HPLC: high-performance liquid chromatography, HPTLC: high-performance thin layer chromatography, Rh B: rhodamine B, and RSD: relative standard deviation.

can be favorable for an analytical method in terms of improving LOD or reducing interference effects from other matrix components. Similarly, the high value of EF (7.43 for FG and 10.77 for Rh B) displays a more efficient extraction. EF is used to assess the effectiveness of an extraction process and to evaluate the contaminants in different samples.

According to our statistical data, the applied procedure has some benefits: excellent correlation coefficient, high PF, and good repeatability.

$$\mathrm{PF} = \frac{\text{Total volume of solution}}{\text{Desired volume after extraction process}}, \quad (3)$$

$$\mathrm{EF} = \frac{\text{Slope of DES calibration curve}}{\text{Slope of calibration curve (direct injection)}}. \quad (4)$$

3.5. Effect of Interference Components. Interference effects of Quinoline Yellow and tartrazine as synthetic dyes were studied under optimized conditions. The percent relative error for FG-Quinoline Yellow, FG-tartrazine, Rh B-Quinoline Yellow, and Rh B-tartrazine was achieved as 3.79%, 6.62%, 8.79%, and 4.59%, respectively, that were less than 10%, indicating no serious effects on the separation and assay of dyes using DES [31].

3.6. Analysis of Real Samples. Pastille and lipstick were used as real samples. A standard addition method was applied to plot the calibration curves. The achieved data, HPTLC images, and three-dimensional chromatograms for quantitation of analytes are shown in Table 7 and Figures 4 and 5, respectively. As shown in Figure 4, the value of R_f for FG and Rh B in real samples is similar to those in preconcentrated dyes (Figure 1), which proves the existence of FG and Rh B in pastille and lipstick, respectively. In addition, the achieved data are compatible with three-dimensional chromatograms (obtained from scanner 3) of FG and Rh B, which are depicted in Figure 5. For each dye, the analysis was performed in triplet. Finally, the amounts of FG and Rh B in real samples were found to be 0.01 and 0.55 $\mathrm{mg{\cdot}g^{-1}}$, respectively. The recovery was calculated using the equation of 5 [40], which showed that the matrix effect was not important in the extraction process. Also, the results revealed acceptable recoveries for the quantitation of both analytes (FG and Rh B) in real samples.

$$\text{Recovery} = \frac{(C_{\text{found}} - C_{\text{real}}) * 100}{C_{\text{added}}}. \quad (5)$$

3.7. Comparison of Method with Other Investigations. The proposed method was compared to other investigations for the analysis of FG and Rh B. As shown in Table 8, the current research provided reasonable results. Compared with other studies, RSD % and PF amounts were higher than or comparable to values achieved using other analytical methods, indicating that the current study can be sensitive and accurate for the simultaneous analysis of FG and Rh B.

4. Conclusions

In the current research, an innovative microextraction method (DES) combined with the HPTLC technique for the preconcentration, separation, and determination of two synthetic dyes including FG and Rh B was established. The selection of a mixture of MeOH (20%), ammonia (20%), and ethyl acetate (60%) as the mobile phase in HPTLC analysis displayed good separation (different R_f values) between FG and Rh B. The best conditions for the simultaneous preconcentration of FG and Rh B were investigated using CCD, achieving a pH value of 4.64, salt concentration of 0.35 $\mathrm{mol{\cdot}L^{-1}}$, DES volume of 378 μL, and stirrer time of 15 min. The quantitative analysis for two dyes showed good repeatability (RSD < 5%), high correlation coefficient ($r = 0.998$ for two dyes), low interference, and excellent PF (21.66 for both dyes) and EF (7.43 for FG and 10.77 for Rh B) parameters, which can be suitable for simultaneous detection of FG and Rh B in food, medicine, textile, and cosmetic industries. Also, the analysis of real samples revealed a low serious matrix effect in this procedure. The main advantage of the developed analysis is the application of a green and environmentally friendly extraction solvent. To the best of our knowledge, the proposed method is the first study for the simultaneous preconcentration of FG and Rh B using DES and the determination of dyes *via* HPTLC as a rapid, green, and cheap analytical method. Finally, it can be concluded that due to the possible risk of synthetic dyes for the environment and human health, the developed process is favorable for routine analysis in different industries because of its sensitivity, simplicity, time saving, and expenditure.

Data Availability

The data used to support the results of this study are included within the article.

Additional Points

Highlights. (i) Deep eutectic solvent as a green solvent was successfully applied for simultaneous preconcentration of fast green FCF and rhodamine B. (ii) Deep eutectic solvent coupled with high-performance thin layer chromatography provides low limit of detection for analytes. (iii) High-performance thin layer chromatography is an appropriate technique for simultaneous determination of preconcentrated fast green FCF and rhodamine B.

Conflicts of Interest

The authors declare that they have no conflicts of interest.

Authors' Contributions

Forough Karami was responsible for methodology, preparation of original draft, conceptualization, visualization, and investigation. Ardeshir Shokrollahi was responsible for supervision, conceptualization, review, and project administration.

Acknowledgments

The authors gratefully wish to thank the support of Yasouj University, Iran, and Shiraz University of Medical Sciences, Shiraz, Iran, for this study.

References

[1] M. Kucharska and J. Grabka, "A review of chromatographic methods for determination of synthetic food dyes," *Talanta*, vol. 80, no. 3, pp. 1045–1051, 2010.

[2] A. Kemp, "Food additives and hyperactivity," *British Medical Journal*, vol. 336, no. 7654, 2008.

[3] M. Alesso, G. Bondioli, M. C. Talío, M. O. Luconi, and L. P. Fernández, "Micelles mediated separation fluorimetric methodology for Rhodamine B determination in condiments, snacks and candies," *Food Chemistry*, vol. 134, no. 1, pp. 513–517, 2012.

[4] D. R. Sulistina and S. Martini, "The effect of Rhodamine B on the cerebellum and brainstem tissue of *Rattus norvegicus*," *Journal of Public Health Research*, vol. 9, no. 2, 2020.

[5] A. Yugatama and T. Hapsari, "Analysis of rhodamine B content in "geplak" marketed in yogyakarta city in 2019," *Journal of Physics: Conference Series*, vol. 1912, no. 1, Article ID 12049, 2021.

[6] Y. Zhu, "Recent advances in detection Technologies of synthetic colorants in foods," *Hans Journal of Food and Nutrition Science*, vol. 2, no. 3, pp. 29–37, 2013.

[7] M. A. Ali and S. A. Bashier, "Effect of fast green dye on some biophysical properties of thymocytes and splenocytes of albino mice," *Food Additives & Contaminants*, vol. 23, no. 5, pp. 452–461, 2006.

[8] A. Mittal, D. Kaur, and J. Mittal, "Batch and bulk removal of a triarylmethane dye, Fast Green FCF, from wastewater by adsorption over waste materials," *Journal of Hazardous Materials*, vol. 163, no. 2-3, pp. 568–577, 2009.

[9] Y. Yamini, M. Rezazadeh, and S. Seidi, "Liquid-phase microextraction – the different principles and configurations," *TrAC, Trends in Analytical Chemistry*, vol. 112, pp. 264–272, 2019.

[10] I. Safarik, S. Mullerova, and K. Pospiskova, "Semiquantitative determination of food acid dyes by magnetic textile solid phase extraction followed by image analysis," *Food Chemistry*, vol. 274, pp. 215–219, 2019.

[11] A. Jangju, K. Farhadi, M. Hatami et al., "Application of zein-modified magnetite nanoparticles in dispersive magnetic micro-solid-phase extraction of synthetic food dyes in foodstuffs," *Journal of Separation Science*, vol. 40, no. 6, pp. 1343–1352, 2017.

[12] A. Asfaram, M. Ghaedi, and A. Goudarzi, "Optimization of ultrasound-assisted dispersive solid-phase microextraction based on nanoparticles followed by spectrophotometry for the simultaneous determination of dyes using experimental design," *Ultrasonics Sonochemistry*, vol. 32, pp. 407–417, 2016.

[13] T. Sun, M. Wang, D. Wang, and Z. Du, "Solid-phase microextraction based on nickel-foam@polydopamine followed by ion mobility spectrometry for on-site detection of Sudan dyes in tomato sauce and hot-pot sample," *Talanta*, vol. 207, Article ID 120244, 2020.

[14] C. Yu, Q. Liu, L. Lan, and B. Hu, "Comparison of dual solvent-stir bars microextraction and U-shaped hollow fiber–liquid phase microextraction for the analysis of Sudan dyes in food samples by high-performance liquid chromatography–ultraviolet/mass spectrometry," *Journal of Chromatography A*, vol. 1188, no. 2, pp. 124–131, 2008.

[15] H. Badiee, M. A. Zanjanchi, A. Zamani, and A. Fashi, "Hollow fiber liquid-phase microextraction based on the use of a rotating extraction cell: a green approach for trace determination of rhodamine 6G and methylene blue dyes," *Environmental Pollution*, vol. 255, Article ID 113287, 2019.

[16] B. Chen and Y. Huang, "Dispersive liquid-phase microextraction with solidification of floating organic droplet coupled with high-performance liquid chromatography for the determination of Sudan dyes in foodstuffs and water samples," *Journal of Agricultural and Food Chemistry*, vol. 62, no. 25, pp. 5818–5826, 2014.

[17] K. Sharafi, N. Fattahi, M. Pirsaheb, H. Yarmohamadi, and M. Fazlzadeh Davil, "Trace determination of lead in lipsticks and hair dyes using microwave-assisted dispersive liquid–liquid microextraction and graphite furnace atomic absorption spectrometry," *International Journal of Cosmetic Science*, vol. 37, no. 5, pp. 489–495, 2015.

[18] S. N. Shah, F. Uzcan, and M. Soylak, "Ultrasound-assisted deep eutectic solvent microextraction procedure for traces Ponceau 4R in water and cosmetic samples," *International journal of Environmental Science and Technology*, vol. 19, no. 1, pp. 189–196, 2022.

[19] S. V. Smirnova, K. A. Lyskovtseva, and I. V. Pletnev, "Extraction and determination of synthetic food dyes using tetraalkylammonium based liquid-liquid extraction," *Microchemical Journal*, vol. 162, Article ID 105833, 2021.

[20] A. Shokrollahi, H. B. Pili, and K. H. Doust, "Microspectrophotometric determination of erythrosine in beverage and water samples after ultrasonic assisted supramolecular-based dispersion solidification liquid–liquid microextraction,"

Journal of Analytical Chemistry, vol. 72, no. 6, pp. 617–623, 2017.

[21] A. P. Abbott, D. Boothby, G. Capper, D. L. Davies, and R. K. Rasheed, "Deep eutectic solvents formed between choline chloride and carboxylic acids: versatile alternatives to ionic liquids," *Journal of the American Chemical Society*, vol. 126, no. 29, pp. 9142–9147, 2004.

[22] F. Aydin, E. Yilmaz, and M. Soylak, "Vortex assisted deep eutectic solvent (DES)-emulsification liquid-liquid microextraction of trace curcumin in food and herbal tea samples," *Food Chemistry*, vol. 243, pp. 442–447, 2018.

[23] M. Rizwan, R. Yahya, A. Hassan et al., "pH sensitive hydrogels in drug delivery: brief history, properties, swelling, and release mechanism, material selection and applications," *Polymers*, vol. 9, no. 12, p. 137, 2017.

[24] J. Chen, Y. Li, X. Wang, and W. Liu, "Application of deep eutectic solvents in food analysis: a Review," *Molecules*, vol. 24, no. 24, p. 4594, 2019.

[25] C. Ruß and B. König, "Low melting mixtures in organic synthesis-an alternative to ionic liquids?" *Green Chemistry*, vol. 14, no. 11, pp. 2969–2982, 2012.

[26] Z. Gholami, M. H. Marhamatizadeh, S. Yousefinejad, M. Rashedinia, and S. M. Mazloomi, "Vortex-assisted dispersive liquid-liquid microextraction based on hydrophobic deep eutectic solvent for the simultaneous identification of eight synthetic dyes in jellies and drinks using HPLC-PDA," *Microchemical Journal*, vol. 170, Article ID 106671, 2021.

[27] M. Faraji, "Determination of some red dyes in food samples using a hydrophobic deep eutectic solvent-based vortex assisted dispersive liquid-liquid microextraction coupled with high performance liquid chromatography," *Journal of Chromatography A*, vol. 1591, pp. 15–23, 2019.

[28] A. Dalmaz and S. Sivrikaya Özak, "Green deep eutectic solvent assisted liquid–liquid microextraction procedure for Sunset Yellow dye in effervescent vitamin C tablets," *Journal of the Iranian Chemical Society*, vol. 19, no. 6, pp. 2359–2366, 2022.

[29] E. Yilmaz and M. Soylak, "A novel and simple deep eutectic solvent based liquid phase microextraction method for rhodamine B in cosmetic products and water samples prior to its spectrophotometric determination," *Spectrochimica Acta Part A: Molecular and Biomolecular Spectroscopy*, vol. 202, pp. 81–86, 2018.

[30] Q. Han, Y. Sun, K. Shen, Y. Yan, and X. Kang, "Rapid determination of seven synthetic dyes in casual snacks based on packed-fibers solid-phase extraction coupled with HPLC-DAD," *Food Chemistry*, vol. 347, Article ID 129026, 2021.

[31] K. Zhang, C. Liu, S. Li, Y. Wang, G. Zhu, and J. Fan, "Vortex-assisted liquid-liquid microextraction based on a hydrophobic deep eutectic solvent for the highly efficient determination of Sudan i in food samples," *Analytical Letters*, vol. 53, no. 8, pp. 1204–1217, 2020.

[32] W. Wu, S. Liu, T. Guo et al., "Rapid screening of 70 colorants in dyeable foods by using ultra-high-performance liquid chromatography–hybrid quadrupole–orbitrap mass spectrometry with customized accurate-mass database and mass spectral library," *Food Chemistry*, vol. 356, Article ID 129643, 2021.

[33] A. Shokrollahi and T. Roozestan, "CPE-Scanometry as a new technique for the determination of dyes: application for the determination of fast green FCF dye and comparison with spectrophotometric results," *Analytical Methods*, vol. 5, no. 18, pp. 4824–4831, 2013.

[34] A. Shokrollahi and F. D. Kashkoli, "Determination of violet covasol as a cosmetic dye in water samples by a CPE-Scanometry method," *Chinese Chemical Letters*, vol. 27, no. 5, pp. 659–665, 2016.

[35] B. Milz, P. Schnurr, J. Grafmüller, K. Oehler, and B. Spangenberg, "A validated quantification of Sudan red dyes in spicery using TLC and a 16-bit flatbed scanner," *Journal of AOAC International*, vol. 101, no. 5, pp. 1397–1401, 2019.

[36] F. Karami, S. Jaberi, A. Afsari, and M. Moein, "Quantitation of rosmarinic acid and caffeic acid in various *Salvia* genera by high performance thin layer chromatography," *Trends in Pharmaceutical Sciences*, vol. 6, no. 3, pp. 205–212, 2020.

[37] M. Tomczyk, A. Bazylko, and J. Bonarewicz, "Method development and validation for optimized separation of quercetin derivatives in selected Potentilla species using high-performance thin-layer chromatography photodensitometry method," *Journal of Pharmaceutical and Biomedical Analysis*, vol. 61, pp. 265–270, 2012.

[38] A. K. Sakira, M. S. M. J. Ouattara, M. Yabre, M. Bande, and T. I. Some, "Contribution to the detection of poor quality sildenafil drugs in Burkina Faso using high-performance thin-layer chromatography," *Journal of Analytical Methods in Chemistry*, vol. 2021, Article ID 4093859, 9 pages, 2021.

[39] Y. Liu, T. A. Brettell, J. Victoria, M. R. Wood, and M. E. Staretz, "High performance thin-layer chromatography (HPTLC) analysis of cannabinoids in cannabis extracts," *Forensic Chemistry*, vol. 19, Article ID 100249, 2020.

[40] A. Shokrollahi and F. Karami, "Preconcentration of phenylalanine in cheese and yoghurt using deep eutectic solvent and determination by HPLC technique," *Current Analytical Chemistry*, vol. 19, no. 3, pp. 272–280, 2023.

[41] A. P. Nambiar, M. Sanyal, and P. S. Shrivastav, "Simultaneous densitometric determination of eight food colors and four sweeteners in candies, jellies, beverages and pharmaceuticals by normal-phase high performance thin-layer chromatography using a single elution protocol," *Journal of Chromatography A*, vol. 1572, pp. 152–161, 2018.

[42] A. Safavi, R. Ahmadi, and A. M. Ramezani, "Vortex-assisted liquid-liquid microextraction based on hydrophobic deep eutectic solvent for determination of malondialdehyde and formaldehyde by HPLC-UV approach," *Microchemical Journal*, vol. 143, pp. 166–174, 2018.

[43] P. Li, P. Zhao, W. Liu et al., "Determination of common ginsenosides in Kang'ai injection by aqueous two-phase extraction with deep eutectic solvents and HPLC-UV/DAD," *Microchemical Journal*, vol. 137, pp. 302–308, 2018.

[44] J. Werner, "Novel deep eutectic solvent-based ultrasounds-assisted dispersive liquid-liquid microextraction with solidification of the aqueous phase for HPLC-UV determination of aromatic amines in environmental samples," *Microchemical Journal*, vol. 153, Article ID 104405, 2020.

[45] R. Zhang, M. Hummelgård, G. Lv, and H. Olin, "Real time monitoring of the drug release of rhodamine B on graphene oxide," *Carbon*, vol. 49, no. 4, pp. 1126–1132, 2011.

[46] B. Renger, Z. Végh, and K. Ferenczi-Fodor, "Validation of thin layer and high performance thin layer chromatographic methods," *Journal of Chromatography A*, vol. 1218, no. 19, pp. 2712–2721, 2011.

[47] N. Pourreza, S. Rastegarzadeh, and A. Larki, "Micelle-mediated cloud point extraction and spectrophotometric determination of rhodamine B using Triton X-100," *Talanta*, vol. 77, no. 2, pp. 733–736, 2008.

[48] Y. Yu and Z. Fan, "Determination of rhodamine B in beverages using a polystyrene-coated magnetite nanocomposite for magnetic solid phase extraction," *Analytical Letters*, vol. 49, no. 12, pp. 1835–1846, 2016.